



Original Paper

Differences in and factors controlling organic matter enrichment in the Ziliujing Formation shale in the Sichuan Basin



Peng Li ^{a, b, c, *}, Zhong-Bao Liu ^{a, b, c}, He Bi ^{d, **,} Tao Jiang ^e, Rui-Kang Bian ^{a, b, c}, Peng-Wei Wang ^{a, b, c}, Xiao-Yu Shang ^f

^a State Key Laboratory of Shale Oil and Gas Enrichment Mechanisms and Efficient Development, Beijing, 102206, China

^b Key Laboratory of Shale Oil/Gas Exploration and Production Technology, SINOPEC, Beijing, 102206, China

^c Petroleum Exploration and Production Research Institute, SINOPEC, Beijing, 102206, China

^d Research Institute of Petroleum Exploration and Development, PetroChina, Beijing, 100083, China

^e Chinese Academy of Geological Sciences, Beijing, 100037, China

^f No.4 Oil Production Plant in Daqing Oilfield Co Ltd., Daqing, 163511, Heilongjiang, China

ARTICLE INFO

Article history:

Received 24 August 2022

Received in revised form

4 March 2023

Accepted 25 October 2023

Available online 28 October 2023

Edited by Jie Hao and Teng Zhu

Keywords:

Lacustrine shale

Ziliujing Formation

Sichuan Basin

Enrichment mechanism of organic matter

ABSTRACT

Lacustrine shale oil and gas are important fields for unconventional exploration and development in China, and organic-rich shale deposition lays down the critical foundation for hydrocarbon generation. There are two sets of shale, the Dongyuemiao and Da'anzhai Members, in the Ziliujing Formation in the Sichuan Basin. To identify the differential enrichment characteristics of organic matter and clarify its controlling factors, geochemical analyses of organic and inorganic geochemical analyses were performed. The results showed that the total organic carbon content of the Dongyuemiao shale (1.36%) is slightly higher than that of the Da'anzhai shale (0.95%). The enrichment of organic matter in the two shales resulted from the comprehensive controls of paleoproductivity, paleoenvironment, and terrigenous input, but different factors have different effects. In addition, driven by climate, the change in the sulfate concentration in the bottom water further led to the different intensities of bacterial sulfate reduction in early diagenesis. This made a great difference regarding organic matter accumulation in the two members. In general, climate may have played a dominant role in organic matter enrichment in the two sets of shale.

© 2023 The Authors. Publishing services by Elsevier B.V. on behalf of KeAi Communications Co. Ltd. This is an open access article under the CC BY-NC-ND license (<http://creativecommons.org/licenses/by-nc-nd/4.0/>).

1. Introduction

As the United States is changing its energy strategy through the use of shale oil and gas, a revolutionary wave has swept the globe (Jin et al., 2019). As the third country to realize commercial exploitation of shale oil and gas after the United States and Canada, China has been making great efforts in the exploration and development of shale oil and gas (Dai et al., 2014; Feng et al., 2016, 2020; Nie et al., 2018). The Sichuan Basin is the birthplace of shale gas innovation in China. In addition to the typical marine shale of the Wufeng-Longmaxi Formation, there are multiple layers of

lacustrine organic-rich shale in the Sichuan Basin, especially the shales in the Jurassic Dongyuemiao and Da'anzhai Members, Ziliujing Formation. Potential hydrocarbon resources have been confirmed in these two members by previous studies (Xu et al., 2017a; Liu et al., 2020; Li et al., 2021; Xiao et al., 2021).

Organic-rich shale is not only the material basis for oil and gas generation, but also a significant reservoir, which is the target for the exploration and development of shale oil and gas (Tourtelot, 1979; Klemme and Ulmishek, 1991; Cai et al., 2007). Therefore, organic-rich shale formations have attracted significant attention from researchers (Zou et al., 2015, 2019; Liu et al., 2020). When considering the enrichment mechanism of organic matter, there has always been controversy between 'preservation theory' and 'productivity theory'. 'Productivity theory' holds that high paleoproductivity and resulting oceanic anoxic conditions control the deposition of organic-rich materials (Herbin et al., 1995; Perkins et al., 2008). 'Preservation theory' believes that the deposition of

* Corresponding author.

** Corresponding author.

E-mail addresses: lipeng2017.syky@sinopec.com (P. Li), bihe@petrochina.com.cn (H. Bi).

organic matter is more the result of anoxic water and emphasizes the important influence of an anoxic depositional environment on the enrichment of organic matter (Hatch and Leventhal, 1992; Wignall and Hallam, 1992). Compared to marine shale, lacustrine shale develops in a more complex sedimentary environment, and its organic matter enrichment mechanism is more susceptible to paleoenvironment perturbation (Liu et al., 2020). Previous studies suggest that the global climate was warm during the Jurassic period, and studies in different regions have revealed significant responses to global climate events (Hallam et al., 1993; Xiao et al., 2021). In particular, the Toarcian oceanic anoxic event (T-OAE) occurred during the Early Jurassic (Hesselbo et al., 2000; McElwain et al., 2005; Svensen et al., 2007; Xu et al., 2017b; Ruebsam et al., 2018; Liu et al., 2020). This event also had a significant impact on terrestrial ecosystems, corresponding to the depositional period of the Da'anzhai Member, whereas the Dongyuemiao Member shale deposition was not affected by global climate events (Xu et al., 2017b).

The two sets of organic-rich shale in the Dongyuemiao section and Da'anzhai Members were both deposited in semideep lake facies. Total organic carbon (TOC) values are mainly between 0.5% and 2.0%, with a maximum of 4.0% and an average of more than 1%. The organic matter types are II₁, II₂ and III, mainly II₁ and II₂ (Li et al., 2013, 2022; Xu et al., 2017b; Liu et al., 2022a, 2022b). Previous studies suggest that the anoxic deep water, high terrestrial inputs, and weak weathering were conducive to the rapid deposition and preservation of lacustrine organic matter (Wang et al., 2020). However, previous researchers have not systematically analyzed the differences in the geochemical characteristics of the two sets of shale, especially the differences in organic matter enrichment and its influential factors.

To investigate the influence of paleoclimatic change on organic-rich shales, the shales in the Dongyuemiao and Da'anzhai Members of the Ziliujing Formation in the Sichuan Basin were studied. TOC and total sulfur (TS) analyses combined with major and trace element analyses were used to identify the paleoenvironment while introducing a sulfate reduction index (SRI) to quantify the relative strength of bacterial sulfate reduction (BSR). This study discusses the influence of oceanic anoxic events on the formation of lacustrine organic-rich shale and clarifies the relationship between organic matter depletion and efficient preservation during the formation of organic-rich shale. These results provide a reference for evaluating the characteristics of lacustrine organic-rich shales.

2. Geological setting

The Sichuan Basin is located on the northwest margin of the Yangtze Plate, which is surrounded by a series of orogenic belts (Liu et al., 2013, 2016; Feng et al., 2016). The formation and evolution of the basin and sedimentary processes are coupled with the activities of the surrounding orogenic belt (Liu et al., 2001). The Late Triassic witnessed a transition to a terrestrial sedimentary environment in the Sichuan Basin. Following the Indosinian movement, the Longmen and Daba Mountains were successively uplifted. In the Early Jurassic, the basin mainly experienced lacustrine deposition and entered the foreland basin evolution stage, forming a steep pattern in the north and a gentle pattern in the south (Li et al., 2013).

The Jurassic strata in the Sichuan Basin are mainly clastic sediments, with total thicknesses of 2000–4400 m. The stratigraphic units from bottom to top are the Lower Jurassic Ziliujing, Middle Jurassic Lianggaoshan and Shaximiao, and Upper Jurassic Suining and Penglaizhen Formations. The Ziliujing Formation is 100–600 m thick, and it is thinner in the western part of the basin and gradually thicker toward the east (Li et al., 2013; Wang et al., 2018; Liu et al., 2022a). According to the vertical lithologic assemblages, four

members can be delineated from bottom to top: Zhenzhuchong, Dongyuemiao, Maanshan and Da'anzhai (Fig. 1).

The Dongyuemiao Member is thin, with thicknesses ranging from 5 to 50 m, but its lithologic distribution is stable. The lower part mainly consists of gray to dark gray micrite, shell limestone, and marl with black shale. The upper part is mainly composed of gray, grayish green, and dark purple shale and multiple thin-bedded marly and shell limestone lenses. These shales bear abundant freshwater bivalve fossils that are found in shallow to semi-deep lake (Li et al., 2021; Liu et al., 2022b).

The lithology and thickness of the Da'anzhai Member vary significantly. In the northern Sichuan Basin, the Da'anzhai Member mainly consists of dark gray shale and shell limestone, with subordinate thin marl and siltstone, with relatively large thicknesses ranging from 100 to 160 m. In the central and southern Sichuan Basin, magenta and yellow-green shales gradually increase and are frequently interbedded with thin silt-fine sandstones, whereas the lenticular form of shell limestone decreases, and its thickness is reduced to 40–80 m (Xiao et al., 2021; Li et al., 2022). The freshwater bivalves and ostracod fossils in this lithologic segment are the most abundant and widely distributed in the Ziliujing Formation, and the continuous deposition of freshwater bivalves often formed thick massive shell beach deposits with a large-area banded ring distribution (Xu et al., 2017b). On the landward side of the shell beach, mottled argillaceous deposits of lake shore-shallow lake facies were deposited. Basinward, deep-semideep lacustrine black shale deposits formed, and the thickness correspondingly increases (Wang et al., 2020).

3. Materials and methods

To systematically study the organic matter enrichment characteristics of shale in the Jurassic Ziliujing Formation, systematic coring was carried out in three wells, Wells F1 and X101 in the Fuling area, and Well Y4 in the Yuanba area. A total of 32 samples were obtained, including 18 and 14 clay-rich mudstone and shale samples from the Dongyuemiao and Da'anzhai Members, respectively. Each core sample was ground into powder, with mesh sizes of 80–100 (sieve pore diameter of 180–150 μm). The experiments in this study were conducted at the Wuxi Research Institute of the SINOPEC Petroleum Exploration and Development Research Institute. We selected 25 samples for TOC and TS content analyses, which were determined using a CS-230 carbon-sulfur analyzer. Prior to measurement, the samples were treated with hydrochloric acid to remove carbonate. Thirty-two samples were selected for element analyses to evaluate the paleoclimate, paleosalinity, redox conditions and terrestrial input. A VISTA MPX inductively coupled plasma emission spectrometer and X II inductively coupled plasma mass spectrometer (ICP-MS) were used. Major elements were measured using the wavelength dispersion method after powdered samples were fused into glass beads. Trace elements were measured after sample powder was acid-digested using HNO₃ and HF.

4. Results and discussion

4.1. TOC and TS variability

In this study, TOC and TS distributions in the Dongyuemiao and Da'anzhai shales in the Sichuan Basin were compared with those in euxinic (Black Sea), normal marine, and freshwater lake sediments (Fig. 2) (Bernier and Raiswell, 1983). First, comparisons among the euxinic, normal marine, and freshwater sediments showed that the distribution of TOC in the freshwater sediment was greatly scattered, with a variation range of 0.12%–8.88%, averaging 3.65%. The

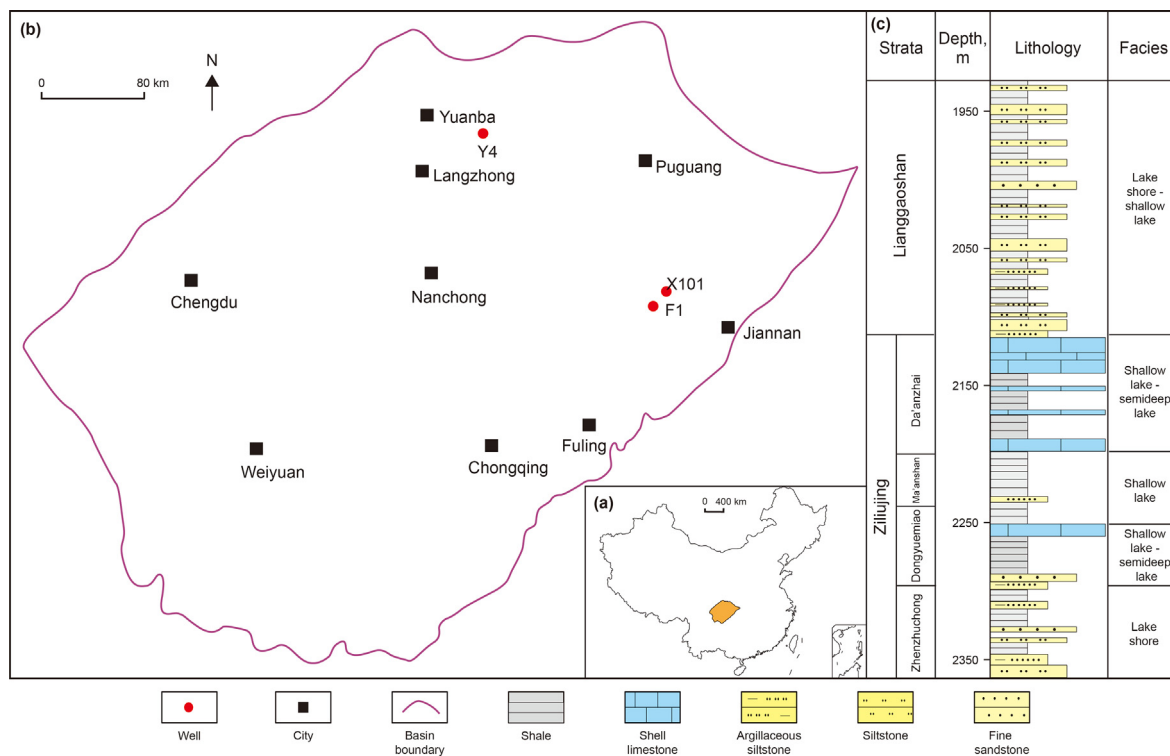


Fig. 1. Location and geological context of the study area. (a) Location map of the Sichuan Basin. (b) Sampling well locations. (c) Stratigraphic section of the Jurassic strata in the Sichuan Basin.

TOC distribution in the euxinic sediment was similar to that in the normal marine sediment at 0.18%–5.08% and 0.28%–5.34%, averaging 2.10% and 1.79%, respectively. The TS contents in freshwater lake sediment were very low, ranging from 0.03% to 0.45%, with an average TS content of 0.15%. The TS values of normal marine and euxinic sediment were 0.36%–1.77% and 0.11%–1.79%, respectively, and were evidently higher than those in freshwater sediment. The TOC contents in the Dongyuemiao shale were 0.35%–3.03%, with an average of 1.32%, and the TOC contents in the Da'anzhai shale were 0.22%–1.51%, with an average of 0.93%, which was significantly lower than that in the Dongyuemiao shale (Table 1). The TS contents in the Dongyuemiao shale ranged from 0 to 0.23%, with an average of only 0.07%. However, the TS contents in the Da'anzhai shale were higher, ranging from 0.04% to 1.73%, with an average of 0.49% (Fig. 2). By comparison, the TOC content of the Dongyuemiao shale was similar to that of normal marine sediment, but significantly lower than that of freshwater sediment, and its TS content was similar to that of freshwater sediment. The TOC content of the

Da'anzhai shale was lower than that of all modern sediments, while its TS content was similar to that of normal marine sediment and significantly higher than that of freshwater sediment.

4.2. Primary productivity and organic matter accumulation

Paleoproductivity is an important factor in organic-rich accumulation and determines the original organic matter content. The accumulation rate of barite (BaSO₄) in sediments is positively related to primary productivity (Dymond et al., 1992; Paytan et al., 1996). To reduce the dilution of terrigenous inputs, the Ba/Al ratio is often used to qualitatively evaluate paleoproductivity (Algeo and Maynard, 2004). The Ba/Al ratio of the Dongyuemiao Member ranged from 17.06–44.87 × 10⁻⁴, with an average of 33.85 × 10⁻⁴, and that of the Da'anzhai Member ranged from 24.81–56.31 × 10⁻⁴, with an average of 37.76 × 10⁻⁴ (Table 2). We also conducted a Z-Test on the two groups of data, and the result was 0.424, which is less than 1.96, with no significant difference.

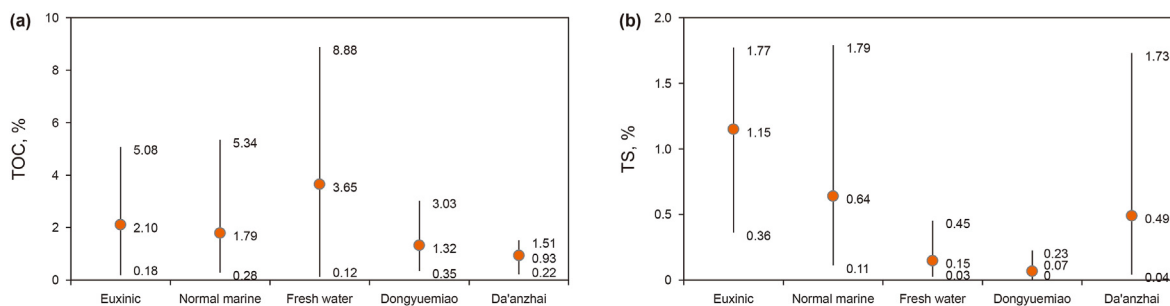


Fig. 2. TOC and TS variability in different settings (after Berner and Raiswell, 1983). (a) The average TOC contents of the Ziliujing shale are lower than those of modern sediments. (b) The TS contents of shale in the Dongyuemiao Member are similar to those of freshwater sediments, and the TS contents of shale in the Da'anzhai Member are similar to those of normal marine sediments.

Table 1
TOC and TS contents of the Ziliujing shale in the Sichuan Basin.

Samples	Well	Depth, m	Strata	TOC, %	TS, %	SRI
2	F1	2736.30	J1d	1.33	0.10	1.05
4	F1	2712.96	J1d	1.64	0.23	1.10
6	X101	2294.33	J1d	0.58	0.01	1.02
9	X101	2275.55	J1d	1.97	0.09	1.03
10	X101	2275.53	J1d	1.96	0.10	1.04
11	X101	2274.20	J1d	1.84	0.11	1.04
13	X101	2269.69	J1d	1.46	0.16	1.08
14	Y4	4053.90	J1d	0.68	0.01	1.01
15	Y4	4051.81	J1d	0.64	0.00	1.00
19	Y4	4012.28	J1d	0.35	0.00	1.01
20	Y4	4008.42	J1d	1.16	0.02	1.01
22	Y4	3997.17	J1d	3.03	0.05	1.01
23	Y4	3985.42	J1d	0.52	0.01	1.01
25	F1	2661.90	J1da	0.47	0.12	1.19
26	F1	2635.77	J1da	0.68	0.10	1.11
28	F1	2622.76	J1da	0.22	0.04	1.14
30	F1	2603.40	J1da	1.51	0.31	1.15
31	F1	2598.32	J1da	1.24	1.73	2.05
38	X101	2149.77	J1da	0.85	0.83	1.74
44	Y4	3790.14	J1da	0.88	0.18	1.15
45	Y4	3786.53	J1da	0.70	0.14	1.15
46	Y4	3760.75	J1da	1.31	0.75	1.43
48	Y4	3754.39	J1da	0.78	0.42	1.41
49	Y4	3752.63	J1da	1.33	0.41	1.23
51	Y4	3748.23	J1da	1.23	0.83	1.51

The Ba/Al distributions of these two shales were similar, indicating similar paleoproductivity characteristics. A fan-shaped positive correlation between TOC and Ba/Al is shown in Fig. 3. As the Ba/Al ratio increased, TOC tended to increase, but the correlation was not obvious. Xiao et al. (2021) also found that there was no correlation between TOC and Ba/Al in the Da'anzhai shale. Therefore, for the two sets of shale in the Ziliujing Formation, biological productivity was not the main factor controlling organic matter enrichment.

4.3. Sedimentary environment characteristics and organic matter accumulation

4.3.1. Paleoclimate

Mn often exists as Mn^{2+} in lakes. When Mn^{2+} reaches saturation in water, it precipitates (Liu et al., 2022). Therefore, the high Mn content in the sediments indicates arid and hot paleoclimatic conditions. Conversely, stable Mn levels indicate a relatively warm and wet climate. In humid climates, Fe precipitates as $Fe(OH)_3$ colloids. Therefore, a high Fe/Mn ratio indicates a warm and humid climate, whereas a correspondingly low Fe/Mn ratio indicates a hot and dry climate (Reheis, 1990; Xu et al., 2021; Liu et al., 2022). The Fe/Mn ratios in the shales from three wells in the Dongyuemiao Member were 46.85–253.06, with an average value of 125.94 (Table 2). The Fe/Mn ratios in the Da'anzhai Member were 35.32–143.65, with an average value of 96.05 (Table 2), which is evidently lower than that in the Dongyuemiao Member, indicating that the paleoclimate changed from warm and humid to arid and hot from the Dongyuemiao Member to the Da'anzhai Member. Moreover, the large variations in the Fe/Mn ranges also indicate that the depositional environment of the two strata were not invariable but experienced climatic fluctuations. Xu et al. (2017b) by comparing the organic carbon isotopes confirmed that the Da'anzhai Member responded to the Toarcian oceanic anoxic event. This global climate event may have affected the terrestrial ecosystem, leading to a relatively arid and hot climate. However, Fig. 4 shows no obvious correlation between the TOC content and Fe/Mn ratio of the Dongyuemiao and Da'anzhai shales, indicating that the impact of climate change on the enrichment of organic matter was also not very significant.

4.3.2. Paleosalinity

In a natural water medium, Sr migrates farther than Ba under the same conditions. When freshwater mixes with saltwater, Ba^{2+} in freshwater combines with SO_4^{2-} in saltwater to form $BaSO_4$, which then precipitates. However, $SrSO_4$ is highly soluble and can migrate further and precipitate under biological action (Mcarthur et al., 2008; Allmen et al., 2010; Paiste et al., 2020). Thus, the Sr/Ba ratio increases with increasing distance from the lakeshore. Generally, the Sr/Ba ratio is less than 1 in freshwater and greater than 1 in saltwater (Wang et al., 2021). The Sr/Ba ratios of the Dongyuemiao Member ranged from 0.17 to 0.82, with an average value of 0.24 (Table 2). The Sr/Ba ratios of the Da'anzhai Member ranged from 0.19 to 0.75, with an average value of 0.36 (Table 2). The salinity of the lake water increased during the deposition of the Da'anzhai Member.

As the water salinity increases, the MgO content increases and the Al_2O_3 content decreases. Therefore, the MgO/Al_2O_3 ratio can be used to indicate the change in the salinity of the water medium. When the water medium salinity increases, the MgO/Al_2O_3 ratio has a high value, and vice versa (Adegoke et al., 2014; Wei and Algeo, 2019). From the Dongyuemiao Member to the Da'anzhai Member, the MgO/Al_2O_3 ratio gradually increases, indicating that the water salinity gradually increased, which is the same finding as the interpreted Sr/Ba result (Table 2). The change in the paleosalinity has a certain synergy with the paleoclimate, which may be due to the global drought caused by oceanic anoxic events. The arid climate enhances the evaporation of water and leads to an increase in water salinity. Moreover, the Da'anzhai Member may have experienced transgression, and seawater intrusion affected the change in the water salinity in the lacustrine basin (Xu et al., 2017b).

Fig. 5 shows that TOC content has no clear relationship with the Sr/Ba and MgO/Al_2O_3 ratios, but the values of the different layers are zoned. Overall, the salinity of the Da'anzhai Member is stronger than that of the Dongyuemiao Member, but the TOC content is lower than that of the Dongyuemiao Member, indicating that the paleosalinity of water may have an impact on the organic matter enrichment.

4.3.3. Paleoredox conditions

The paleoredox conditions reflect the oxygen content of the lake water during the depositional period. V, Ni and Cr are sensitive to redox changes in the sedimentary environment and reflect the paleoenvironment redox conditions (Algeo and Maynard, 2004; Tribovillard et al., 2006). High $V/(V + Ni)$ values (0.84–0.89) indicate water stratification and the existence of an anaerobic H_2S environment in the bottom water. Medium values (0.54–0.82) indicate an anaerobic environment with insignificant stratification. Low values (0.46–0.60) reflect weak stratification and anoxic environments. A V/Cr ratio greater than 4.25 indicates a reducing environment, a ratio less than 2.0 indicates an oxidizing environment, and a ratio between 2.0 and 4.25 indicates a weakly oxidizing and weakly reducing environment (Dill, 1986; Hatch and Leventhal, 1992; Jones and Manning, 1994). During the deposition of Cu and Zn, deposition differentiation occurred with the difference in the oxygen content in the environment, and the Cu/Zn ratio was positively correlated with the oxygen content (Tribovillard et al., 2006; Chen et al., 2019; Algeo and Liu, 2020).

The results from the analysis of different redox indicators show certain differences (Table 2). The $V/(V + Ni)$ ratios of the Dongyuemiao Member ranged from 0.57 to 0.89, with an average value of 0.77, reflecting anoxic and anaerobic sedimentary environments. The V/Cr ratios ranged from 0.49 to 1.99, with an average value of 1.38. The Cu/Zn ratios ranged from 0.08 to 0.48, with an average value of 0.34. The Ni/Co ratios ranged from 1.82 to 7.13, with an

Table 2
Elemental geochemical indicators of the Dongyuemiao and Da'anzhai shale.

Samples	Depth, m	Strata	Well	Ba/Al, $\times 10^{-4}$	Fe/Mn	Sr/Ba	MgO/Al ₂ O ₃	Cu/Zn	V/(V + Ni)	Ni/Co	V/Cr	Al, %	Zr, $\times 10^{-6}$
2	2736.30	J1d	F1	41.15	101.47	0.22	0.10	0.40	0.76	3.11	1.55	10.39	198.86
4	2712.96	J1d	F1	39.96	143.93	0.20	0.10	0.40	0.77	3.32	1.62	10.84	139.48
6	2294.33	J1d	X101	29.22	63.97	0.23	0.10	0.27	0.76	2.14	1.52	8.06	320.47
7	2293.43	J1d	X101	28.05	54.54	0.41	0.11	0.08	0.73	2.18	0.77	5.12	139.56
8	2291.85	J1d	X101	17.06	253.06	0.82	0.12	0.15	0.89	1.96	1.99	8.31	137.91
9	2275.55	J1d	X101	44.87	143.09	0.21	0.10	0.44	0.76	3.18	1.57	10.17	175.33
10	2275.53	J1d	X101	39.72	75.78	0.20	0.10	0.38	0.78	3.23	1.57	9.46	166.91
11	2274.20	J1d	X101	39.08	137.89	0.22	0.10	0.47	0.77	3.07	1.66	9.92	187.90
13	2269.69	J1d	X101	39.85	118.52	0.17	0.10	0.37	0.77	3.12	1.60	10.62	157.71
14	4053.90	J1d	Y4	37.62	203.33	0.19	0.04	0.48	0.81	7.13	1.45	10.07	279.84
15	4051.81	J1d	Y4	30.87	93.53	0.17	0.07	0.41	0.81	3.23	1.95	10.42	253.82
17	4020.70	J1d	Y4	34.32	83.38	0.17	0.07	0.23	0.72	3.85	0.49	5.61	532.40
18	4015.76	J1d	Y4	32.31	160.20	0.20	0.07	0.43	0.74	3.96	0.60	6.48	483.10
19	4012.28	J1d	Y4	32.49	141.93	0.19	0.07	0.46	0.79	3.01	1.32	9.43	206.16
20	4008.42	J1d	Y4	29.72	200.27	0.20	0.08	0.25	0.57	1.82	0.89	8.26	316.19
21	4003.78	J1d	Y4	29.82	46.85	0.19	0.08	0.36	0.79	2.82	1.27	6.70	186.72
22	3997.17	J1d	Y4	31.08	190.12	0.18	0.05	0.29	0.80	2.89	1.71	10.77	175.94
23	3985.42	J1d	Y4	32.17	55.11	0.18	0.10	0.33	0.77	3.08	1.24	7.93	260.77
25	2661.90	J1da	F1	40.55	95.40	0.27	0.13	0.41	0.73	2.82	1.20	8.23	209.72
26	2635.77	J1da	F1	32.07	76.93	0.32	0.11	0.39	0.75	2.83	1.37	9.86	158.40
27	2631.33	J1da	F1	24.81	133.15	0.49	0.13	0.39	0.74	1.99	1.44	8.80	154.47
28	2622.76	J1da	F1	27.73	35.32	0.44	0.14	0.36	0.76	2.65	1.50	7.99	120.55
30	2603.40	J1da	F1	34.73	128.86	0.31	0.10	0.40	0.77	3.40	1.54	9.49	154.49
31	2598.32	J1da	F1	34.32	143.03	0.27	0.12	0.46	0.77	2.42	1.55	9.13	140.48
34	2158.25	J1da	X101	34.69	139.14	0.50	0.11	0.34	0.78	3.38	1.68	8.87	120.68
38	2149.77	J1da	X101	56.31	133.61	0.75	0.14	0.19	0.75	2.76	1.54	7.55	108.97
44	3790.14	J1da	Y4	40.12	63.39	0.24	0.10	0.44	0.76	2.69	1.55	9.25	190.24
45	3786.53	J1da	Y4	35.87	59.30	0.26	0.11	0.40	0.75	2.23	1.41	7.17	252.35
46	3760.75	J1da	Y4	44.06	78.52	0.39	0.10	0.37	0.77	2.63	1.46	7.27	171.79
48	3754.39	J1da	Y4	40.99	143.65	0.19	0.10	0.35	0.80	3.22	1.77	10.50	176.88
49	3752.63	J1da	Y4	39.16	67.62	0.29	0.11	0.41	0.75	2.68	1.58	8.61	194.68
51	3748.23	J1da	Y4	43.25	46.80	0.31	0.11	0.41	0.76	3.02	1.65	8.75	172.93

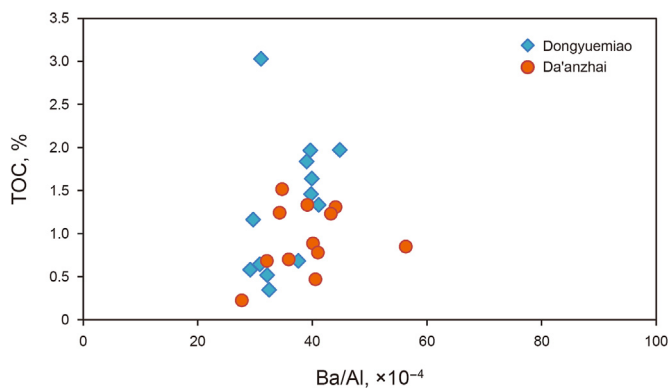


Fig. 3. Bivariate plot of Ba/Al and TOC. The samples of the Dongyuemiao and Da'anzhai Members are scattered, and there are no evident zoning characteristics.

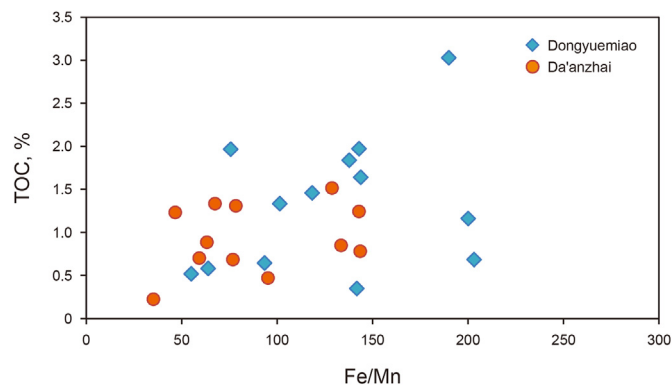


Fig. 4. Bivariate plot of Fe/Mn and TOC. The samples of the Da'anzhai Member are surrounded by those of the Dongyuemiao Member, indicating that the climate change of the Da'anzhai Member was not as strong as that of the Dongyuemiao Member.

average value of 3.17, indicating an oxygen-rich environment (Table 2). The Da'anzhai Member had similar characteristics, with V/(V + Ni) ratios ranging from 0.73 to 0.80, and an average value of 0.76, indicating an anaerobic sedimentary environment. The V/Cr ratios ranged from 1.20 to 1.77, with an average value of 1.52. The Cu/Zn ratios ranged from 0.19 to 0.46, with an average value of 0.38. The Ni/Co ratio ranged from 1.99 to 3.40, with an average value of 2.77 (Table 2). Overall, these characteristics indicate an oxygenated sedimentary environment.

Fig. 6 shows that the TOC in both sets of shale has no evident correlation with the V/Cr, Cu/Zn, and Ni/Co ratios, indicating that the redox environment may not clearly influence the organic enrichment of lacustrine shale.

4.4. Terrigenous input and organic matter accumulation

Al, Zr, and other elements in shale are often used to indicate terrigenous input (Rachold and Brumsack, 2001; Calvert and Pedersen, 2007). The Al contents in the Dongyuemiao Member were 5.12–10.84%, with an average value of 8.81%, and the Zr contents were 137.91–532.40 $\times 10^{-6}$, with an average value of 239.95 $\times 10^{-6}$ (Table 2). The Al contents of the Da'anzhai Member ranged from 7.17% to 10.50%, with an average value of 8.68%, and the Zr content ranged from 108.97 to 252.35 $\times 10^{-6}$ (Table 2), with an average value of 166.19 $\times 10^{-6}$. The Al and Zr contents of shale in the Dongyuemiao Member were significantly higher than those in the Da'anzhai Member, indicating a more terrigenous source input for the Dongyuemiao Member, which may be one of the reasons for

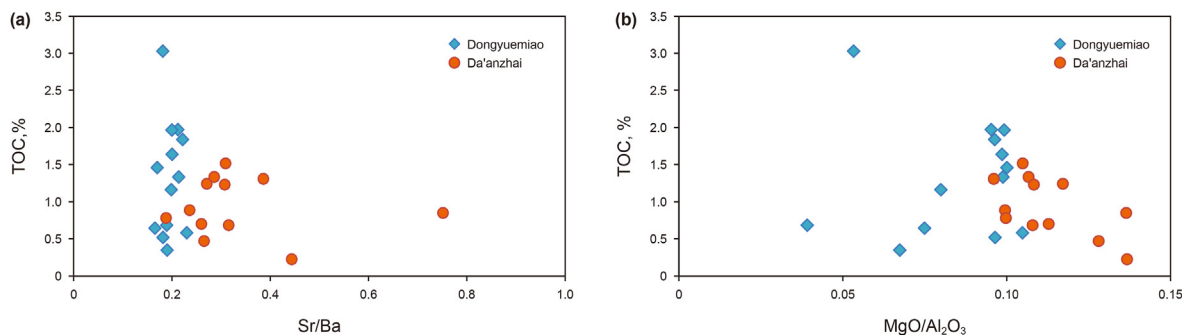


Fig. 5. Bivariate plot of Sr/Ba, MgO/Al₂O₃, and TOC. Overall, the paleosalinity of the Da'anzhai Member is slightly higher than that of the Dongyuemiao Member.

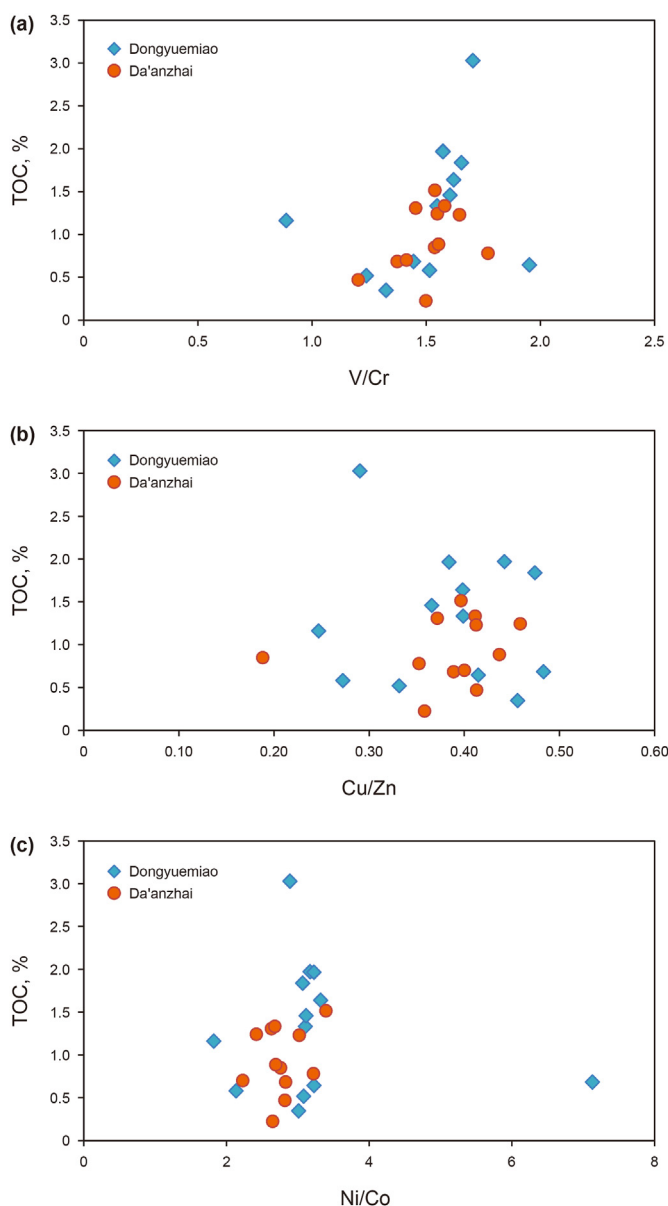


Fig. 6. Bivariate plots of Ni/Co, Cu/Zn, V/Cr, and TOC. There is no evident difference in redox conditions between samples from the Dongyuemiao and Da'anzhai Members.

the difference in the organic matter abundance between these two members.

As shown in Fig. 7, the relationship between the TOC and Al and Zr contents of two sets of shale in the Ziliujing Formation is inconsistent. TOC tends to increase with increasing Al content, but has no obvious correlation with the Zr content, indicating that the impact of terrestrial input on organic matter enrichment is complex. With the increase in terrigenous materials, the nutrients carried by terrigenous materials also increase, and the improved paleoproductivity is conducive to the enrichment of organic matter, but the input of terrigenous materials also dilutes the organic matter of primary sediments, resulting in a reduction in the organic matter content.

This comprehensive study shows that both the Dongyuemiao and Da'anzhai shales have high paleoproductivity characteristics. The climate during the Dongyuemiao Member deposition was relatively humid, whereas the dry climate during the deposition of the Da'anzhai Member led to a significantly higher salinity than that of the Dongyuemiao Member. The shales in the Dongyuemiao and Da'anzhai Members were deposited in an oxygen-rich environment. The shale in the Dongyuemiao Member had more terrigenous input than that in the Da'anzhai Member, which has a dual effect on the enrichment of organic matter. Thus, the enrichment of organic matter in these two shales is the result of the comprehensive control of the paleoproductivity, paleoenvironment, and terrigenous input. However, different factors have different effects, and climate-driven environmental differences may be the fundamental reason for the differences between the two members.

4.5. C–S relationship and BSR

In addition to the element indexes used to analyze the paleosedimentary environment, the C–S relationship can also be used to assess the aqueous environment. The consumption of the original sedimentary organic matter by BSR in the early diagenetic stage can be analyzed through the C–S relationship, and the mechanism of organic matter enrichment can be further discussed.

Under ideal conditions, early diagenesis specifically includes aerobic respiration, nitrate reduction, metal (iron, manganese) oxide reduction, sulfate reduction and methanogenesis (Hesse and Schacht, 2011). Through calculations, Thullner et al. (2013) found that the relative contribution of sulfate reduction to organic matter mineralization could reach 76%. Therefore, this study focused on analyzing the influence of sulfate reduction on organic matter enrichment.

Berner (1984) found that the organic carbon and sulfur in modern sediments have special changing rules, and the depositional environment can be distinguished by the ratio of organic carbon to sulfur. Berner and Raiswell (1983) and Leventhal (1995) proposed that TOC/TS values less than 2.0, between 2.0 and 3.6,

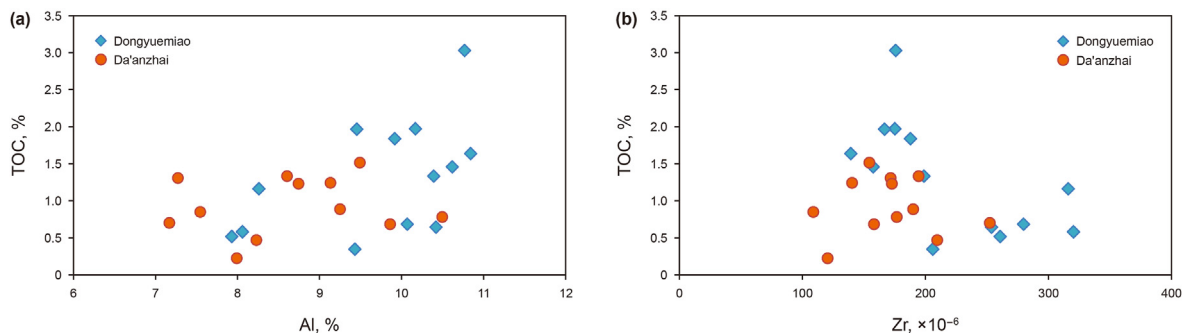


Fig. 7. Bivariate plot of Al, Zr, and TOC. There is no evident difference in the terrigenous input between samples from the Dongyuemiao and Da'anzhai Members.

and greater than 10 represent sulfide environments and sediments deposited under euxinic, normal marine, and freshwater conditions. Organic-rich sediments deposited in the geologic past can also be used to characterize the paleowater environment (Leventhal, 1995; Jones and Fike, 2013; Alsenz et al., 2015; Cao et al., 2016; Liu et al., 2021).

The cross-plot analysis of TOC and TS (Fig. 8) reveals that the corresponding environments of the Da'anzhai and Dongyuemiao shales were evidently different. The TOC/TS ratios of the Dongyuemiao shale are generally greater than 10, suggesting largely freshwater deposition, while the TOC/TS ratios of the Da'anzhai shale are mostly less than 10, and many values are less than 2, indicating brackish water deposition. These results show that the sulfate concentrations in the sedimentary water of the two shales were different. The sulfate concentration in the Da'anzhai shale is obviously higher than that in the Dongyuemiao shale, which is similar to previous results obtained from Sr/Ba and MgO/Al₂O₃. It is speculated that regional climate change may be caused by oceanic anoxic events and that a relatively dry climate enhanced evaporation in the lake basin and increased water salinity.

To characterize the effect of sulfate reduction on organic matter, the SRI is used to express the intensity of sulfate reduction. The SRI evaluates the residual organic carbon content (Lallier-Verges et al., 1993). The initial organic carbon content is the degraded organic carbon after sulfate reduction plus the residual organic carbon (Eq. (1)).

$$SRI = (TOC + C_{loss}) / TOC \tag{1}$$

where C_{loss} represents the amount of organic carbon degraded in sulfate reduction. The residual organic carbon content is a

percentage of TOC, while the degraded organic carbon content is calculated by dividing the percentage of TS by 1.33 according to the sulfate reduction equation (Eq. (2)) stoichiometry proposed by Berner (1984):

$$C_{loss} = S(\%) / 1.33 \tag{2}$$

The stronger BSR is, the higher the SRI value. The calculation of the SRI index is based on the assumption that all hydrogen sulfide produced by BSR is precipitated by sulfide in specific sediments, without considering the process of hydrogen sulfide being oxidized again. Therefore, the SRI should be considered the lowest degradation-consumption index of organic carbon relative to the real consumption of organic matter by BSR (Liu et al., 2021).

The SRI values of the Dongyuemiao and Da'anzhai shales were different in the distribution range, as shown by the clear zoning in the cross-plot (Fig. 9). The SRI values of the Dongyuemiao shale samples ranged from 1 to 1.35, with an average of 1.08. The overall values were less than 1.375, and TOC did not change with the SRI index. The SRI values of the Da'anzhai shale ranged from 1.11 to 2.05, with an average of 1.41. When the SRI values were greater than 1.375, TOC decreased with an increase in the SRI.

These results suggest that differences in the aqueous environment have an evident controlling effect on the enrichment of organic matter. The climate of shale deposition in the Dongyuemiao Member was relatively warm and humid, and terrigenous material input promoted improved paleoproductivity. Although some of the consumed organic matter was consumed by oxygen-rich water, abundant organic matter was still deposited. Later in the early diagenetic stage, freshwater depositional environments had a limited sulfate content, which restricted its role in organic matter

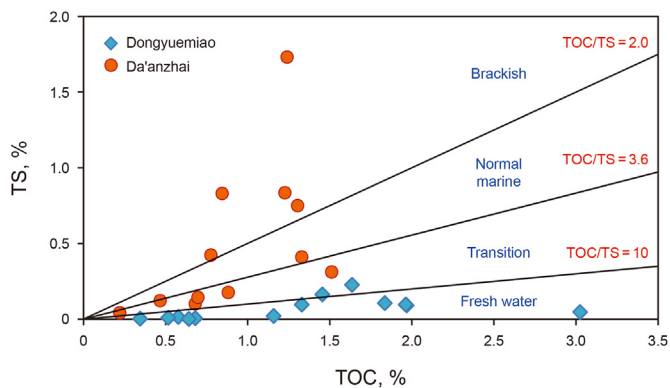


Fig. 8. Bivariate plot of TOC and TS (after Liu et al., 2021). The samples of the Dongyuemiao Member are mainly located in the freshwater area, while the samples of the Da'anzhai Member are distributed in the transition and brackish zones.

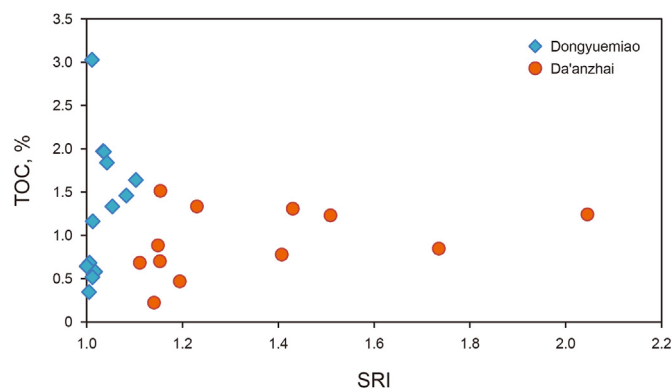


Fig. 9. Bivariate plot of SRI and TOC. The SRI value of the samples from the Da'anzhai Member are higher than those of the Dongyuemiao Member, indicating more intense BSR.

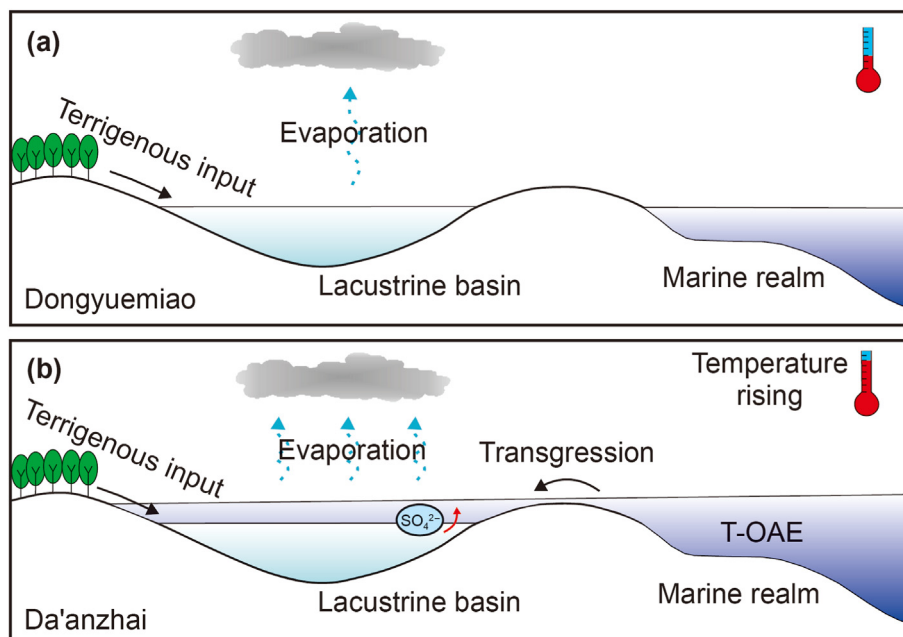


Fig. 10. Model diagram of the influence of the environment on the sulfate concentration in the lake basin in different periods. (a) During the depositional period of the Dongyuemiao Member, the lake basin was isolated from the ocean, deposition was mainly controlled by the regional climate, evaporation was weak, and there was no additional sulfate input, showing the characteristics of freshwater lakes. The original deposited organic matter had not been consumed by strong sulfate reduction and was effectively preserved with a high TOC. (b) During the depositional period of the Da'anzhai Member, affected by the T-OAE event, the lake basin was connected with the ocean, and sulfate-rich seawater poured into the lake basin. At the same time, evaporation intensified, which further increased the sulfate concentration in the water body. As a result, the original sedimentary organic matter was subjected to strong sulfate reduction, which broke the original balance between preservation and consumption, and the TOC was low.

consumption. The SRI remained low. More original sedimentary organic matter was preserved, which eventually formed an organic-rich shale with high TOC and low TS contents in the Dongyuemiao Member (Fig. 10a).

The sedimentary period of the Da'anzhai shale was affected by the oceanic anoxic event, and the climatic conditions were relatively hot and dry, with intense evaporation. The evaporation capacity was greater than the rainfall and surface runoff, which condensed the lake and increased its salinity. The paleoproductivity of the Da'anzhai Member was similar to that of the Dongyuemiao Member, and their redox conditions and terrigenous input were not significantly different. Therefore, the difference in organic matter enrichment may have been influenced by early diagenesis. Owing to the relatively high water salinity in the Da'anzhai Member, the water sulfate concentration increased and intensified the BSR effect; increased amounts of the original sedimentary organic matter were consumed. These analyses are consistent with the low TOC and high TS contents of the shale in the Da'anzhai Member (Fig. 10b).

5. Conclusions

The TOC contents of the Dongyuemiao shale are 0.35%–3.03%, with an average of 1.32%, which is equivalent to that of normal marine sediments, but significantly lower than that of modern freshwater sediments. The TOC contents of the Da'anzhai shale range from 0.22% to 1.51%, with an average of only 0.93%, which is lower than that of the Dongyuemiao member. However, its TS content is high, which is equivalent to that of normal marine sediments.

The enrichment of organic matter in the two sets of shale is the result of the comprehensive control of the paleoproductivity, paleoenvironment, and terrigenous inputs, but different factors have different effects. The Dongyuemiao shale experienced high

paleoproductivity and a relatively humid climate. More terrigenous inputs have a dual effect on the enrichment of organic matter, which may promote increased paleoproductivity and dilute organic matter. The shale in the Da'anzhai Member also had high paleoproductivity; however, because of the dry climate, the water salinity was significantly higher than that in the Dongyuemiao Member.

The difference in the aqueous environment driven by the climate also had an evident controlling effect on the enrichment of organic matter. During the sedimentary period of the Dongyuemiao Member, the water salinity was low, and the low sulfate concentration restricted BSR. Therefore, the original sedimentary organic matter was preserved to a greater extent, forming shale with high TOC and low TS contents. However, the high salinity and high sulfate concentration of the water body during the shale deposition of the Da'anzhai Member exacerbated the BSR effect to a certain extent, and original sedimentary organic matter was consumed to a greater extent, forming shale with relatively low TOC and high TS contents.

Declaration of competing interest

The manuscript 'Differences in and factors controlling organic matter enrichment in the Ziliujing Formation shale in the Sichuan Basin' has not been previously published and not been currently submitted for review to other journals. The authors declare that they have no known competing financial interests or personal relationships that could have appeared to influence the work reported in this paper.

Acknowledgments

This work was funded by the National Natural Science Foundation of China (Grant No. 42002139 and U20B6001) and the

Strategic Priority Research Program of the Chinese Academy of Sciences (Grant No. XDA14010404).

References

- Adegoke, A.K., Abdullah, W.H., Hakimi, M.H., et al., 2014. Geochemical characterization of Fika Formation in the Chad (Bornu) basin, northeastern Nigeria: implications for depositional environment and tectonic setting. *Appl. Geochem.* 43, 1–12. <https://doi.org/10.1016/j.apgeochem.2014.01.008>.
- Algeo, T.J., Maynard, J.B., 2004. Trace-element behavior and redox facies in core shales of Upper Pennsylvanian Kansas-type cyclothems. *Chem. Geol.* 206 (3–4), 289–318. <https://doi.org/10.1016/j.chemgeo.2003.12.009>.
- Algeo, T.J., Liu, J.S., 2020. A re-assessment of elemental proxies for paleoredox analysis. *Chem. Geol.* 540, 119549. <https://doi.org/10.1016/j.chemgeo.2020.119549>.
- Allmen, K., Böttcher, M.E., Samankassou, E., et al., 2010. Barium isotope fractionation in the global barium cycle: first evidence from barium minerals and precipitation experiments. *Chem. Geol.* 277 (1/2), 70–77. <https://doi.org/10.1016/j.chemgeo.2010.07.011>.
- Alsenz, H., Illner, P., Ashckenazi-Polivoda, S., et al., 2015. Geochemical evidence for the link between sulfate reduction, sulfide oxidation and phosphate accumulation in a late cretaceous upwelling system. *Geochem. Trans.* 16 (2), 1–13. <https://doi.org/10.1186/s12932-015-0017-1>.
- Berner, R.A., Raiswell, R., 1983. Burial of organic carbon and pyrite sulfur in sediments over Phanerozoic time: a new theory. *Geochem. Cosmochim. Acta* 47, 855–862. [https://doi.org/10.1016/0016-7037\(83\)90151-5](https://doi.org/10.1016/0016-7037(83)90151-5).
- Berner, R.A., 1984. Sedimentary pyrite formation: an update. *Geochem. Cosmochim. Acta* 48 (4), 605–615. [https://doi.org/10.1016/0016-7037\(84\)90089-9](https://doi.org/10.1016/0016-7037(84)90089-9).
- Calvert, S.E., Pedersen, T.F., 2007. Elemental proxies for palaeoclimatic and palaeoceanographic variability in marine sediments: interpretations and applications. *Dev. Mar. Geol.* 1, 567–644. [https://doi.org/10.1016/S1572-5480\(07\)01019-6](https://doi.org/10.1016/S1572-5480(07)01019-6).
- Cao, H.S., Kaufman, A.J., Shan, X.L., et al., 2016. Sulfur isotope constraints on marine transgression in the lacustrine upper cretaceous Songliao Basin, northeastern China. *Palaeogeogr. Palaeoclimatol.* 451, 152–163. <https://doi.org/10.1016/j.palaeo.2016.02.041>.
- Cai, J.G., Bao, Y.J., Yang, S.Y., et al., 2007. Research on preservation and enrichment mechanisms of organic matter in muddy sediment and mudstone. *Sci. China E* 50, 765–775. <https://doi.org/10.1007/s11430-007-0005-0>.
- Chen, G., Gang, W.Z., Liu, Y.Z., et al., 2019. Organic matter enrichment of the Late Triassic Yanchang Formation (Ordos Basin, China) under dysoxic to oxic conditions: insights from pyrite framboid size distributions. *J. Asian Earth Sci.* 170, 106–117. <https://doi.org/10.1016/j.jseae.2018.10.027>.
- Dai, J.X., Zou, C.N., Liao, S.M., et al., 2014. Geochemistry of the extremely high thermal maturity Longmaxi shale gas, southern Sichuan Basin. *Org. Geochem.* 74, 3–12. <https://doi.org/10.1016/j.orggeochem.2014.01.018>.
- Dill, H., 1986. Metallogenesis of early paleozoic graptolite shales from the graefenthal horst (northern bavaria-federal-republic-of-Germany). *Econ. Geol.* 81 (4), 889–903. <https://doi.org/10.2113/gsecongeo.81.4.889>.
- Dymond, J., Suess, E., Lyle, M., 1992. Barium in deep-sea sediment: a geochemical proxy for paleoproductivity. *Paleoceanography* 7 (2), 163–181. <https://doi.org/10.1029/92PA00181>.
- Feng, Z.Q., Liu, D., Huang, S.P., et al., 2016. Carbon isotopic composition of shale gas in the silurian Longmaxi Formation of the changing area, Sichuan Basin. *Petrol. Explor. Dev.* 43 (5), 769–777. [https://doi.org/10.1016/S1876-3804\(16\)30092-1](https://doi.org/10.1016/S1876-3804(16)30092-1).
- Feng, Z.Q., Hao, F., Dong, D.Z., et al., 2020. Geochemical anomalies in the lower silurian shale gas from the Sichuan Basin, China: insights from a Rayleigh-type fractionation model. *Org. Geochem.* 142, 103981. <https://doi.org/10.1016/j.orggeochem.2020.103981>.
- Hallam, A., Crame, J.A., Manceñido, M.O., et al., 1993. Jurassic climates as inferred from the sedimentary and fossil record [and discussion]. *Philos. T. R. Soc. B* 341 (1297), 287–296. <https://doi.org/10.1098/rstb.1993.0114>.
- Hatch, J.R., Leventhal, J.S., 1992. Relationship between inferred redox potential of the depositional environment and geochemistry of the upper Pennsylvanian (missourian) Stark shale member of the dennis limestone, Wabaunsee county, Kansas. *Chem. Geol.* 99, 65–82. [https://doi.org/10.1016/0009-2541\(92\)90031-Y](https://doi.org/10.1016/0009-2541(92)90031-Y).
- Herbin, J.P., Fernandez-Martinez, J.L., Geysant, J.R., et al., 1995. Study of the kimberidge/tithonian in the northwest European shelf. *Mar. Petrol. Geol.* 12 (2), 177–194. [https://doi.org/10.1016/0264-8172\(95\)92838-n](https://doi.org/10.1016/0264-8172(95)92838-n).
- Hesse, R., Schacht, U., 2011. Early diagenesis of deep-sea sediments. *Dev. Sedimentol.* 63, 557–713. <https://doi.org/10.1016/B978-0-444-53000-4.00009-3>.
- Hesselbo, S.P., Gröcke, D.R., Jenkyns, H.C., et al., 2000. Massive dissociation of gas hydrate during a Jurassic oceanic anoxic event. *Nature* 406, 392–395. <https://doi.org/10.1038/35019044>.
- Jin, J.J., Bai, Z.R., Gao, B., et al., 2019. Has China ushered in the shale oil and gas revolution? *Oil Gas Geol.* 40 (3), 5–12. <https://doi.org/10.11743/ogg20190301>.
- Jones, B., Manning, D.A.C., 1994. Comparison of geochemical indexes used for the interpretation of palaeoredox conditions in ancient mudstones. *Chem. Geol.* 111, 111–129. [https://doi.org/10.1016/0009-2541\(94\)90085-X](https://doi.org/10.1016/0009-2541(94)90085-X).
- Jones, D.S., Fike, D.A., 2013. Dynamic sulfur and carbon cycling through the end-Ordovician extinction revealed by paired sulfate–pyrite $\delta^{34}\text{S}$. *Earth Planet Sci. Lett.* 363, 144–155. <https://doi.org/10.1016/j.epsl.2012.12.015>.
- Klemme, H.D., Ulmishke, G.F., 1991. Effective petroleum source rocks of the world: stratigraphic distribution and controlling depositional factors. *AAPG Bull.* 75, 1809–1851. <https://doi.org/10.1306/0C9B2A47-1710-11D7-8645000102C1865D>.
- Lallier-Verges, E., Bertrand, P., Desprairies, A., 1993. Organic matter composition and sulfate reduction intensity in Oman Margin sediments. *Mar. Geol.* 112, 57–69. [https://doi.org/10.1016/0025-3227\(93\)90161-N](https://doi.org/10.1016/0025-3227(93)90161-N).
- Leventhal, J.S., 1995. Carbon-sulfur plots to show diagenetic and epigenetic sulfidation in sediments. *Geochem. Cosmochim. Acta* 59 (6), 1207–1211. [https://doi.org/10.1016/0016-7037\(95\)00036-Y](https://doi.org/10.1016/0016-7037(95)00036-Y).
- Li, P., Liu, Z.B., Nie, H.K., et al., 2021. Heterogeneity characteristics of lacustrine shale oil reservoir under the control of lithofacies: a case study of the Dongyuemiao Member of Jurassic Ziliujing Formation, Sichuan Basin. *Front Earth Sc-SWITZ.* 9, 736544. <https://doi.org/10.3389/feart.2021.736544>.
- Li, Q.W., Liu, Z.B., Chen, F.R., et al., 2022. Geochemical characteristics and organic matter provenance of shale in the jurassic Da'anzhai member, northeastern Sichuan Basin. *Front Earth Sc-SWITZ.* 10, 860477. <https://doi.org/10.3389/feart.2022.860477>.
- Li, Y.J., Feng, Y.Y., Liu, H., et al., 2013. Geological characteristics and resource potential of lacustrine shale gas in the Sichuan Basin, SW China. *Petrol. Explor. Dev.* 40 (4), 454–460. [https://doi.org/10.1016/S1876-3804\(13\)60057-9](https://doi.org/10.1016/S1876-3804(13)60057-9).
- Liu, J., Chen, Q.Z., Yang, Y.X., et al., 2022. Coupled redox cycling of Fe and Mn in the environment: the complex interplay of solution species with Fe- and Mn-(oxyhydr) oxide crystallization and transformation. *Earth Sci. Rev.* 232, 104105. <https://doi.org/10.1016/j.earscirev.2022.104105>.
- Liu, M., Sun, P., Them, R., T. R., et al., 2020. Organic geochemistry of a lacustrine shale across the toarcian oceanic anoxic event (early jurassic) from NE China. *Global Planet. Change* 191, 103214. <https://doi.org/10.1016/j.gloplacha.2020.103214>.
- Liu, Q.Y., Worden, R.H., Jin, Z.J., et al., 2013. TSR versus non-TSR processes and their impact on gas geochemistry and carbon stable isotopes in Carboniferous, Permian and Lower Triassic marine carbonate gas reservoirs in the Eastern Sichuan Basin, China. *Geochem. Cosmochim. Acta* 100 (1), 96–115. <https://doi.org/10.1016/j.gca.2012.09.039>.
- Liu, Q.Y., Zhu, D.Y., Jin, Z.J., et al., 2016. Coupled alteration of hydrothermal fluids and sulfate reduction (TSR) in ancient dolomite reservoirs – an example from Sinian Dengying Formation in Sichuan Basin, southern China. *Precambrian Res.* 285, 39–57. <https://doi.org/10.1016/j.precamres.2016.09.006>.
- Liu, Q.Y., Li, P., Jin, Z.J., et al., 2021. Preservation of organic matter in shale linked to bacterial sulfate reduction (BSR) and volcanic activity under marine and lacustrine depositional environments. *Mar. Petrol. Geol.* 127, 104950. <https://doi.org/10.1016/j.marpetgeo.2021.104950>.
- Liu, S.G., Zhao, X.K., Luo, Z.L., et al., 2001. Study on the tectonic events in the system of the Longmen mountain - west sichuan foreland basin, China. *J. Chengdu Univ. Technol. (Sci. Technol. Ed.)* 28 (3), 221–230. <https://doi.org/10.3969/j.issn.1671-9727.2001.03.001>.
- Liu, Z.B., Hu, Z.Q., Liu, G.X., et al., 2022a. Source-reservoir coupling characteristics and development model of continental shale: taking the Jurassic Ziliujing Formation in Sichuan Basin as an example. *Marine Origin Petroleum Geology* 27 (3), 271–280. <https://doi.org/10.3969/j.issn.1672-9854.2022.03.005>.
- Liu, Z.B., Hu, Z.Q., Liu, G.X., et al., 2022b. Source–reservoir features and favorable enrichment interval evaluation methods of high mature continental shale: a case study of the Jurassic Dongyuemiao Member in the Fuxing area, eastern Sichuan Basin. *Nat. Gas. Ind.* 42 (10), 11–24. <https://doi.org/10.3787/j.issn.1000-0976.2022.10.002>.
- Mcarthur, J.M., Algeo, T.J., Schootbrugge, B., et al., 2008. Howarth Basinal restriction, black shales, Re-Os dating, and the Early Toarcian (Jurassic) oceanic anoxic event. *Paleoceanography* 23 (4), PA4217. <https://doi.org/10.1029/2008PA001607>.
- McElwain, J.C., Wade-Murphy, J., Hesselbo, S.P., 2005. Changes in carbon dioxide during an oceanic anoxic event linked to intrusion into Gondwana coals. *Nature* 435, 479–482. <https://doi.org/10.1038/nature03618>.
- Nie, H.K., Jin, Z.J., Zhang, J.C., 2018. Characteristics of three organic matter pore types in the Wufeng-Longmaxi shale of the Sichuan Basin, Southwest China. *Sci. Rep-UK* 8 (1), 1071–1098. <https://doi.org/10.1038/s41598-018-25104-5>.
- Paiste, K., Pellerin, A., Zerkle, A.L., et al., 2020. The pyrite multiple sulfur isotope record of the 1.98 Ga Zaonaga Formation: evidence for biogeochemical sulfur cycling in a semi-restricted Basin. *Earth Planet Sci. Lett.* 534 (5), 116092. <https://doi.org/10.1016/j.epsl.2020.116092>.
- Paytan, A., Kastner, M., Chavez, F.P., 1996. Glacial to interglacial fluctuations in productivity in the equatorial pacific as indicated by marine barite. *Science* 274 (5291), 1355–1357. <https://doi.org/10.1126/science.274.5291.1355>.
- Perkins, R.B., Piper, D.Z., Mason, C.E., 2008. Trace-element budgets in the Ohio/Sunbury shales of Kentucky: constraints on ocean circulation and primary productivity in the Devonian-Mississippian Appalachian Basin. *Palaeogeogr. Palaeoclimatol.* 265, 14–29. <https://doi.org/10.1016/j.palaeo.2008.04.012>.
- Rachold, V., Brumsack, H., 2001. Inorganic geochemistry of Albian sediments from the Lower Saxony Basin NW Germany: palaeoenvironmental constraints and orbital cycles. *Palaeogeogr. Palaeoclimatol.* 174, 121–143. [https://doi.org/10.1016/S0031-0182\(01\)00290-5](https://doi.org/10.1016/S0031-0182(01)00290-5).
- Reheis, M.C., 1990. Influence of climate and eolian dust on the major-element chemistry and clay mineralogy of soils in the northern Bighorn Basin. *U.S.A. Catena* 17 (3), 219–248. [https://doi.org/10.1016/0341-8162\(90\)90018-9](https://doi.org/10.1016/0341-8162(90)90018-9).
- Ruebsam, W., Müller, T., Kovács, J., et al., 2018. Environmental response to the early Toarcian carbon cycle and climate perturbations in the northeastern part of the West Tethys shelf. *Gondwana Res.* 59, 144–158. <https://doi.org/10.1016/j.jgr.2018.03.013>.

- Svensen, H., Planke, S., Chevallerier, L., et al., 2007. Hydrothermal venting of greenhouse gases triggering early jurassic global warming. *Earth Planet Sci. Lett.* 256 (3–4), 554–566. <https://doi.org/10.1016/j.epsl.2007.02.013>.
- Thullner, M., Dale, A.W., Regnier, P., 2013. Global-scale quantification of mineralization pathways in marine sediments: a reaction-transport modeling approach. *Geochem. Geophys. Geosy* 11, 12002. <https://doi.org/10.1029/2010GC003409>.
- Tourtletot, H.A., 1979. Black shale-its deposition and diagenesis. *Clay Clay Miner.* 27, 313–321. <https://doi.org/10.1346/CCMN.1979.0270501>.
- Tribovillard, N., Algeo, T.J., Lyons, T., et al., 2006. Trace metals as paleoredox and paleoproductivity proxies: an update. *Chem. Geol.* 232, 12–32. <https://doi.org/10.1016/j.chemgeo.2006.02.012>.
- Wang, A.H., Wang, Z.H., Liu, J.K., et al., 2021. The Sr/Ba ratio response to salinity in clastic sediments of the Yangtze River Delta. *Chem. Geol.* 559, 119923. <https://doi.org/10.1016/j.chemgeo.2020.119923>.
- Wang, X., He, S., Guo, X.W., et al., 2018. The resource evaluation of jurassic shale in north fuling area, eastern Sichuan Basin, China. *Energ. Fuel* 32 (2), 1213–1222. <https://doi.org/10.1021/acs.energyfuels.7b03097>.
- Wang, X.Y., Jin, Z.K., Zhao, J.H., et al., 2020. Depositional environment and organic matter accumulation of Lower Jurassic nonmarine fine-grained deposits in the Yuanba Area, Sichuan Basin, SW China. *Mar. Petrol. Geol.* 116, 104352. <https://doi.org/10.1016/j.marpetgeo.2020.104352>.
- Wei, W., Algeo, T.J., 2019. Elemental proxies for paleosalinity analysis of ancient shales and mudrocks. *Geochem. Cosmochim. Acta* 287, 341–366. <https://doi.org/10.1016/j.gca.2019.06.034>.
- Wignall, P.B., Hallam, A., 1992. Anoxia as a cause of the Permian/Triassic mass extinction: facies evidence from northern Italy and the western United States. *Palaeogeogr. Palaeoclimatol.* 93, 21–46. [https://doi.org/10.1016/0031-0182\(92\)90182-5](https://doi.org/10.1016/0031-0182(92)90182-5).
- Xiao, Z.L., Chen, S.J., Zhang, S.M., et al., 2021. Sedimentary environment and model for lacustrine organic matter enrichment: lacustrine shale of the Early Jurassic Da'anhai Formation, central Sichuan Basin, China. *J. Palaeogeogr.* 10 (4), 584–601. <https://doi.org/10.1016/j.jop.2021.09.002>.
- Xu, C., Shan, X.L., He, W.T., et al., 2021. The influence of paleoclimate and a marine transgression event on organic matter accumulation in lacustrine black shales from the Late Cretaceous, southern Songliao Basin, Northeast China. *Int. J. Coal Geol.* 246, 103842. <https://doi.org/10.1016/j.coal.2021.103842>.
- Xu, Q.L., Liu, B., Ma, Y.S., et al., 2017. Controlling factors and dynamical formation models of lacustrine organic matter accumulation for the Jurassic Da'anhai Member in the central Sichuan Basin, southwestern China. *Mar. Petrol. Geol.* 86, 1391–1405. <https://doi.org/10.1016/j.marpetgeo.2017.07.014>.
- Xu, W.M., Ruhl, M., Jenkyns, H.C., et al., 2017. Carbon sequestration in an expanded lake system during the Toarcian oceanic anoxic event. *Nat. Geosci.* 10, 129–134. <https://doi.org/10.1038/ngeo2871>.
- Zou, C.N., Dong, D.Z., Wang, Y.M., et al., 2015. Shale gas in China: characteristics, challenges and prospects (II). *Petrol. Explor. Dev.* 41, 753–767. [https://doi.org/10.1016/S1876-3804\(15\)30072-0](https://doi.org/10.1016/S1876-3804(15)30072-0).
- Zou, C.N., Zhu, R.K., Chen, Z.Q., et al., 2019. Organic-matter-rich shales of China. *Earth Sci. Rev.* 189, 51–78. <https://doi.org/10.1016/j.earscirev.2018.12.002>.